Kinetics of NOx Absorption into (NH4)2SO3 Solution in an Ammonia-Based Wet Flue Gas Desulfurization Process

7 AUTHORS, INCLUDING:

Xiang Gao
Nanjing University
401 PUBLICATIONS **5,635** CITATIONS

SEE PROFILE

Zhen Du
Zhejiang University
5 PUBLICATIONS **58** CITATIONS

SEE PROFILE

Honglei Ding
Zhejiang University, Shanghai University of E…
6 PUBLICATIONS **64** CITATIONS

SEE PROFILE

energy&fuels

article

Kinetics of NO$_x$ Absorption into (NH$_4$)$_2$SO$_3$ Solution in an Ammonia-Based Wet Flue Gas Desulfurization Process

Xiang Gao,*,[†] Zhen Du,[†] Hong-lei Ding,[†] Zu-liang Wu,[‡] Hao Lu,[‡] Zhong-yang Luo,[†] and Ke-fa Cen[†]

[†]*State Key Laboratory of Clean Energy Utilization, Zhejiang University, Hangzhou 310027, China, and*
[‡]*Department of Environmental Engineering, Zhejiang Gongshang University, Hangzhou 310035, China*

The mass transfer and kinetics of NO$_x$ absorption into (NH$_4$)$_2$SO$_3$ solution, the main compound of an ammonia-based wet flue gas desulfurization process, have been investigated in a double-stirred reactor. Under the experimental conditions, the gas–liquid reaction between NO$_x$ and the (NH$_4$)$_2$SO$_3$ solution without O$_2$ coexisting is controlled mainly by the gas film because the (NH$_4$)$_2$SO$_3$ concentration is higher than 0.05 mol/L. In this case, the absorption rate of NO$_x$ is found to be zero-order with respect to the (NH$_4$)$_2$SO$_3$ concentration. The inlet partial pressure and the oxidation degree ($\Phi = $ NO$_2$/NO$_x$) have an apparent effect on the absorption rate of NO$_x$. In this research, a simplified mathematical calculated model is applied to the simulation of the absorption process. The experimental results demonstrate that the orders of the reaction with respect to the concentration of NO$_x$ (NO$_2$* or NO*) in the gas phase and the reaction rate constants of NO$_x$ (NO$_2$* or NO*) with (NH$_4$)$_2$SO$_3$ are all a function of the oxidation degree. A kinetic equation for total NO$_x$ absorption as a function of the oxidation degree can be obtained, and the calculated value fits the experimental data well.

1. Introduction

The emissions of SO$_2$ and NO$_x$ have been a major environmental concern because of their hazardous effects on human health and the ecosystems,[1] and the removal of SO$_2$ and NO$_x$ from the flue gases has recently become very important to comply with the strict environmental emission standards.[2] Considering the capital investment, the operation cost, and the equipment space, considerable attention has been focused on the simultaneous removal of SO$_2$ and NO$_x$ in the same temperature range in a single reactor.[1,3−5] The ammonia-scrubbing process not only can produce ammonium fertilizer as a nutrient for crops but also can remove NO$_x$; thus, ammonia-based wet flue gas desulfurization have drawn increasing attention in China.[6−8]

In the ammonia-based wet flue gas desulfurization system, (NH$_4$)$_2$SO$_3$ and small amounts of NH$_4$HSO$_3$ coexist in the scrubbing solution without free NH$_3$;[7] therefore, (NH$_4$)$_2$SO$_3$ is the main compound for the absorption of SO$_2$ and NO$_x$. The ammonia-based wet flue gas desulfurization has experienced high SO$_2$ removal efficiency and has been studied by many scholars.[7−10] However, the detailed information on the absorption of NO$_x$ into (NH$_4$)$_2$SO$_3$ solution is not readily available in the literature, and the absorption of NO$_x$ into (NH$_4$)$_2$SO$_3$ solution in an ammonia-based wet flue gas desulfurization process is quite complicated because of numerous parallel and consecutive reactions occurring in the solution.

At present, there are many different studies concerning the wet flue gas denitrification process using water,[11,12] basic solution [NaOH and Ca(OH)$_2$],[11,13−15] aqueous sulfite,[16−19] or other complex component solutions.[2,20−24] Although NO$_x$ in typical flue gas comprises 90−95% NO,[2] the radicals formed during the corona discharge process[25−27] as well as

*To whom correspondence should be addressed. Fax: (86) 571-87951335. E-mail: xgao1@zju.edu.cn.

(1) Deshwal, B. R.; Lee, H. K. *J. Environ. Sci. (Beijing, China)* **2009,** *21,* 155–161.
(2) Long, X.-l.; Xin, Z.-l.; Chen, M.-b.; Li, W.; Xiao, W.-d.; Yuan, W.-k. *Sep. Purif. Technol.* **2008,** *58,* 328–334.
(3) Adewuyi, Y. G.; He, X. D.; Shaw, H.; Lolertpihop, W. *Chem. Eng. Commun.* **1999,** *174,* 21–51.
(4) Sakai, M.; Su, C. L.; Sasaoka, E. *Ind. Eng. Chem. Res.* **2002,** *41,* 5029–5033.
(5) Lee, H. K.; Deshwal, B. R.; Yoo, K. S. *Korean J. Chem. Eng.* **2005,** *22,* 208–213.
(6) Srivastava, R. K.; Jozewicz, W.; Singer, C. *Environ. Prog.* **2001,** *20,* 219–227.
(7) Gao, X.; Ding, H.-l.; Wu, Z.-l.; Du, Z.; Luo, Z.-y.; Cen, K.-f. *Energy Fuels* **2009,** *23,* 5916–5919.
(8) Gao, X.; Ding, H.; Du, Z.; Wu, Z.; Fang, M.; Luo, Z.; Cen, K. *Appl. Energy* **2010,** *87,* 2647–2651.
(9) Hikita, H.; Asai, S.; Tsuji, T. *J. Chem. Eng. Jpn.* **1978,** *11,* 236–238.
(10) Guo, Y. X.; Liu, Z.; Huang, Z.; Liu, Q.; Guo, S. *Ind. Eng. Chem. Res.* **2005,** *44,* 9989–9995.
(11) Kameoka, Y.; Pigford, R. L. *Ind. Eng. Chem. Fundam.* **1977,** *16,* 163–169.
(12) Lee, Y. N.; Schwartz, S. E. *J. Phys. Chem.* **1981,** *85,* 840–848.
(13) Patwardhan, J. A.; Joshi, J. B. *AIChE J.* **2003,** *49,* 2728–2748.
(14) Zhang, X.; Tong, H.; Zhang, H.; Chen, C. *Ind. Eng. Chem. Res.* **2008,** *47,* 3827–3833.
(15) Newman, B. L.; Carta, G. *AIChE J.* **1988,** *34,* 1190–1199.
(16) Littlejohn, D.; Wang, Y. Z.; Chang, S. G. *Environ. Sci. Technol.* **1993,** *27,* 2162–2167.
(17) Tursic, J.; Grgic, I.; Bizjak, M. *Atmos. Environ.* **2001,** *35,* 97–104.
(18) Chen, L.; Lin, J. W.; Yang, C. L. *Environ. Prog.* **2002,** *21,* 225–230.
(19) Shen, C. H.; Rochelle, G. T. *Environ. Sci. Technol.* **1998,** *32,* 1994–2003.
(20) Mao, Y.-P.; Bi, W.; Long, X.-L.; Xiao, W.-D.; Li, W.; Yuan, W.-k. *Sep. Purif. Technol.* **2008,** *62,* 183–191.
(21) Chu, H.; Chien, T. W.; Twu, B. W. *J. Hazard. Mater.* **2001,** *84,* 241–252.
(22) Enami, S.; Hoffmann, M. R.; Colussi, A. J. *J. Phys. Chem. B* **2009,** *113,* 7977–7981.
(23) Shi, Y.; Wang, H.; Chang, S. G. *Environ. Prog.* **1997,** *16,* 301–306.
(24) Shi, Y.; Littlejohn, D.; Chang, S. G. *Ind. Eng. Chem. Res.* **1996,** *35,* 1668–1672.
(25) Wu, Z. L.; Gao, X.; Luo, Z. Y.; Wei, E. Z.; Zhang, Y. S.; Zhang, J. Z.; Ni, M. J.; Cen, K. F. *Energy Fuels* **2005,** *19,* 2279–2286.
(26) Lin, H.; Gao, X.; Luo, Z. y.; Guan, S. p.; Cen, K. f.; Huang, Z. *J. Environ. Sci. (Beijing, China)* **2004,** *16,* 462–465.
(27) Lin, H.; Gao, X.; Luo, Z.; Cen, K.; Huang, Z. *Fuel* **2004,** *83,* 1349–1355.

**Table 1. Rate and Equilibrium Constants for the Gas-Phase Reactions 1 and 2**

reactions	rate and equilibrium constants	reference
1	$K_1 = 6.98 \times 10^{-15} \exp\left(\frac{6866}{T}\right)$	34
2	$K_2 = 4.12 \times 10^{-13} \exp\left(\frac{4869}{T}\right)$	15

additives, such as MnO_4^- [28] and ClO_2^-,[21,29,30] can convert NO into NO_2; thus, these wet denitrification processes refer to the absorption of NO_x with different NO_2/NO ratios. Meanwhile, the absorption of NO_2/NO mixtures involves a number of chemical reactions, and different NO_2/NO ratios can result in a different NO_x absorption efficiency. For the above reasons, it is necessary to further study the kinetics of NO_x absorption into $(NH_4)_2SO_3$ solution at different NO_2/NO ratios.

The main objective in this work is to study NO_x absorption into $(NH_4)_2SO_3$ solution in an ammonia-based wet process. The NO_x partial pressure and the ratio of NO_2/NO are important characteristics of the gas phase, and the $(NH_4)_2SO_3$ concentration is the other important operating parameter. All of these parameters have some influence on the absorption rate of NO_x in the absorption solution. Because of the complicacy of NO_x absorption, a simplified mathematical calculated model is applied to simulate the total absorption process.

2. Model Details

2.1. Gas- and Liquid-Phase Reactions. NO_x is a mixture of several components, and without H_2O_g, NO_x is a mixture of NO_2, NO, N_2O_3, and N_2O_4 in the gas phase for the following reactions:[31]

$$NO + NO_2 \leftrightarrow N_2O_3 \quad (1)$$

$$2NO_2 \leftrightarrow N_2O_4 \quad (2)$$
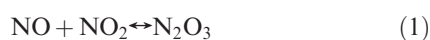
The gas-phase composition of NO_x is characterized by the partial pressures of the two chemical species NO_2^* and NO^*. In addition, the partial pressures of NO_2^* and NO^* are generally defined as follows:[15,31–33]

$$P_{NO_2^*} = P_{NO_2} + P_{N_2O_3} + 2P_{N_2O_4} \quad (3)$$

$$P_{NO^*} = P_{NO} + P_{N_2O_3} \quad (4)$$

$$P_{NO_x} = P_{NO_2^*} + P_{NO^*} \quad (5)$$

The parameter to express the gas composition is the oxidation degree (Φ) defined as[32]

$$\Phi = P_{NO_2^*}/P_{NO_x} \quad (6)$$

Assuming the equilibriums of reactions 1 and 2 in Table 1 throughout the bulk gas phase,[14,32] the partial pressures of N_2O_3 and N_2O_4 are indicated as follows:

$$P_{N_2O_3} = K_1 P_{NO} P_{NO_2} \quad (7)$$

$$P_{N_2O_4} = K_2 P_{NO_2}^2 \quad (8)$$

Combining eqs 7 and 8 with eqs 3 and 4, the following equations are obtained:

$$P_{NO_2^*} = P_{NO_2} + K_1 P_{NO} P_{NO_2} + 2K_2 P_{NO_2}^2 \quad (9)$$

$$P_{NO^*} = P_{NO} + K_1 P_{NO} P_{NO_2} \quad (10)$$

NO_x in the experiment is simulated by mixing two gases of NO and NO_2; therefore, the inlet partial pressures of NO_2^* and NO^* equal the initial partial pressures of NO_2 and NO before they have been mixed or can be calculated by the inlet partial pressures of NO_2 and NO through eqs 9 and 10 in the mixture gas. The outlet partial pressures of NO_2^* and NO^* can also be calculated by the outlet partial pressures of NO_2 and NO through eqs 9 and 10.

Because the concentration of N_2O_3 and N_2O_4 is much lower than that of NO and NO_2, a simplified mathematical calculated model can be developed. In this model, the diffusion and solubility coefficients of NO_2^* and NO^* can approximately equal the diffusion and solubility coefficients of NO_2 and NO, respectively.[15,35]

In the liquid phase, the absorption processes of NO_x into $(NH_4)_2SO_3$ solution involve several reactions. The reactions between NO_2 and the sulfite ion show that NO_2 can oxidize SO_3^{2-} directly; it does not appear to initiate their autoxidation,[16,19,36] and the total absorption path for NO into $(NH_4)_2SO_3$ solution is in the form of nitrogen−sulfur compounds by the reactions between NO and the sulfite ion.[37] Thus, the total reactions of NO_x with $(NH_4)_2SO_3$ solution are given as follows:

$$2NO_2^* + H_2O + SO_3^{2-} \rightarrow 2NO_2^- + SO_4^{2-} + 2H^+ \quad (11)$$

$$NO + SO_3^{2-} \rightarrow NOSO_3^{2-} \quad (12)$$

For a different NO_2/NO ratio, the composition of NO_2^* and NO^* is different. Thus, the NO_2/NO ratio has some influence on the orders of reactions 11 and 12 with respect to the concentration of NO_2^* and NO^* in the gas phase and the reaction rate constants of NO_2^* and NO^* with $(NH_4)_2SO_3$ solution.

2.2. Transport Equations. When the $(NH_4)_2SO_3$ concentration is much larger than the gas-phase concentration at the total reaction cycle, the reactions of NO_2^* and NO^* with $(NH_4)_2SO_3$ can be considered to be the fast irreversible reaction regime according to the theory of absorption with chemical reaction[38] and a double-stirred tank reactor can be used to investigate the characteristics of fast reactions.

In the double-stirred tank reactor, the gas and liquid phases can be considered to be in the completely mixed state.[39] Therefore, the gas-phase component of the outlet gas of the tank can be regarded approximately as that of the inner gas of the tank. In addition, the absorption rates of NO_2^* and NO^* in the gas phase are given by[39]

$$N_A = \frac{v_G P_0}{RTS}\left[\left(\frac{P_A}{P_I}\right)_{in} - \left(\frac{P_A}{P_I}\right)_{out}\right], \quad (A = 1, 2) \quad (13)$$

(28) Chu, H.; Chien, T. W.; Li, S. Y. *Sci. Total Environ.* **2001**, *275*, 127–135.
(29) Chien, T. W.; Chu, H.; Hsueh, H. T. *J. Environ. Eng.* **2003**, *129*, 967–974.
(30) Chien, T. W.; Chu, H. *J. Hazard. Mater.* **2000**, *80*, 43–57.
(31) Pradhan, M. P.; Joshi, J. B. *AlChE J.* **1999**, *45*, 38–50.
(32) De Paiva, J. L.; Kachan, G. C. *Chem. Eng. Process.* **2004**, *43*, 941–948.
(33) De Paiva, J. L.; Kachan, G. C. *Ind. Eng. Chem. Res.* **1998**, *37*, 609–614.

(34) Hofytizer, P. J.; Kwanten, F. J. G. Absorption of nitrous gases. *Process for Air Pollution Control*; CRC Press: Cleveland, OH, 1972.
(35) Thomas, D.; Vanderschuren, J. *Ind. Eng. Chem. Res.* **1997**, *36*, 3315–3322.
(36) Siddiqi, M. A.; Petersen, J.; Lucas, K. *Ind. Eng. Chem. Res.* **2001**, *40*, 2116–2127.
(37) Clifton, C. L.; Altstein, N.; Huie, R. E. *Environ. Sci. Technol.* **1988**, *22*, 586–589.
(38) Danckwerts, P. V. *Gas−Liquid Reactions*; McGraw-Hill: New York, 1970.
(39) Levenspi, O.; Godfrey, J. H. *Chem. Eng. Sci.* **1974**, *29*, 1723–1730.

Then, the total absorption rates of NO_x can be calculated by

$$N_{NO_x} = N_1 + N_2 \qquad (14)$$

The absorption rates of NO_2^* and NO^* into $(NH_4)_2SO_3$ solution are converted to chemical reaction enhancement factors using the following equation according to the two-film model:[24,39]

$$N_A = k_{GA}(P_A - P_{Ai})$$
$$= Ek_{LA}(C_{Ai} - C_{AL}), \quad (A = 1, 2) \qquad (15)$$

According to the phase balance in the gas−liquid interface, $C_{Ai} = P_{Ai}H_A$, the total mass-transfer equation can be expressed by the gas-phase impetus as follows:

$$N_A = \left(P_A - \frac{C_{AL}}{H_A}\right)\Big/\left(\frac{1}{k_{GA}} + \frac{1}{EH_Ak_{LA}}\right),$$
$$(A = 1, 2) \qquad (16)$$

The reactions 11 and 12 can be considered to be a fast irreversible reaction and can be simplified to the following scheme:

$$A + \nu B \rightarrow \text{products} \qquad (17)$$

Thus, assuming that the reactions 11 and 12 are a *m*- and *n*th-order reaction,[38] and $C_{AL} = 0$ in the interface, the enhancement factor E of the reactions can be approximately defined by[8]

$$E = \frac{\gamma_L[(E_\infty - E)/(E_\infty - 1)]^{n/2}}{\tanh\{\gamma_L[(E_\infty - E)/(E_\infty - 1)]^{n/2}\}} \qquad (18)$$

where E_∞ and γ_L can be obtained by

$$E_\infty = 1 + D_{BL}C_{BL}/(D_{AL}C_{Ai}), \quad (A = 1, 2) \qquad (19)$$

$$\gamma_L = \frac{1}{k_{LA}}\left[\frac{2}{m_A + 1}k_{Am,n}D_{LA}C_{Ai}^{m_A - 1}C_{BL}^{n_A}\right]^{1/2},$$
$$(A = 1, 2) \qquad (20)$$

For a fast pseudo-*m*- and *n*th-order reaction, there is $\gamma_L \ll E_\infty$.[38] In this case, $E = (1 + \gamma_L^2)^{1/2}$.

Applying these values to eq 16, the following equation for the absorption rate of NO_2^* and NO^* can be obtained:

$$N_A = \frac{P_A}{\dfrac{1}{k_{GA}} + \dfrac{1}{H_A\sqrt{k_{LA}^2 + \dfrac{2}{m_A + 1}k_{Am,n}D_{LA}C_{Ai}^{m_A - 1}C_{BL}^{n_A}}}},$$
$$(A = 1, 2) \qquad (21)$$

Therefore, the total absorption rate of NO_x can be written as

$$N_A = \frac{P_1}{\dfrac{1}{k_{G1}} + \dfrac{1}{H_1\sqrt{k_{L1}^2 + \dfrac{2}{m_1 + 1}k_{1m,n}D_{L1}C_{1i}^{m_1 - 1}C_{BL}^{n_1}}}}$$
$$+ \frac{P_2}{\dfrac{1}{k_{G2}} + \dfrac{1}{H_2\sqrt{k_{L2}^2 + \dfrac{2}{m_2 + 1}k_{2m,n}D_{L2}C_{2i}^{m_2 - 1}C_{BL}^{n_2}}}} \qquad (22)$$

3. Experimental Section

3.1. Absorption Apparatus. A cross-section of the experimental gas−liquid contactor is shown in Figure 1. The stirred cell is made of 80 mm inner diameter stainless-steel tubing, 70 mm long in the liquid section and 50 mm long in the gas section. In addition, the stirred cell has a water jacket through which water is circulated from a
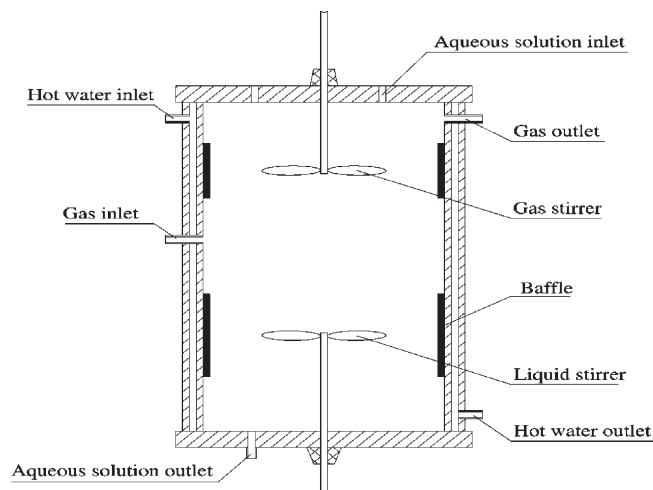

Figure 1. Cross-section of the experimental gas−liquid contactor.

Table 2. All Gases and Chemicals Used in the Experiments

name	specification	manufacturer
N_2	>99.99%	Hangzhou New Century Gas Co., Ltd., China
NO_2	2000 ppm	Hangzhou New Century Gas Co., Ltd., China
NO	2000 ppm	Hangzhou New Century Gas Co., Ltd., China
CO_2	>99.99%	Hangzhou New Century Gas Co., Ltd., China
SO_2	>99.99%/5000 ppm	Hangzhou New Century Gas Co., Ltd., China
$NH_3 \cdot H_2O$	30%	Hangzhou Changzheng Chemical Reagent Co., Ltd., China
NaOH	AR	Sinopharm Chemical Reagent Co., Ltd., China

thermostat to maintain the desired temperature, and the deviation of the temperature is within ±0.5 °C. Four baffles, located 90° apart, are attached to the sides of the gas- and liquid-phase sections. The gas- and liquid-phase sections in the reactor are stirred by a propeller agitator with three flat blades, 8.0 cm in diameter.

All gases and chemicals used in the experiments have been list in Table 2. The $(NH_4)_2SO_3$ solution used in the experiments is made fresh by absorbing pure SO_2 with an aqueous ammonia solution and is diluted with distilled water to obtain the desired concentration. The concentration of the $(NH_4)_2SO_3$ solution is analyzed by an iodimetric technique.

3.2. Experimental Operation. The double-stirred reactor is operated continuously with respect to the gas phase and batchwise with respect to the liquid phase. The continuous gas flow is maintained at about 500 mL/min, and the volume of the aqueous solution in the cell is 350 mL. The gas phase consists of a mixture of NO and NO_2 in nitrogen. NO and NO_2 are supplied from the cylinders and are further diluted with N_2 to the desired concentrations before being fed to the stirred cell. The gas flow rates are controlled by the mass flow meters purchased from SevenStar Huachuang Co., Ltd., China, and the accuracy of the flow rates is ±0.1 mL min^{-1}. Before the gas mixture is fed to the absorber, it is heated to the desired temperature. The liquid phase is the $(NH_4)_2SO_3$ solution and is refreshed after each operation. Continuous stirs for the gas and liquid phase are provided by two separated mechanical agitators.

According to the research of Gu,[40] when the liquid stirring speed is 100−187 rpm and a gas stirring speed is 120−800 rpm,

(40) Gu, Y. X. The chemical absorption process in the disposal of nitric oxide. Thesis, Zhejiang University, Hangzhou, China, 1986.

the gas and liquid phases can be considered to be in the completely mixed state. Thus, the liquid stirring speed is 120 rpm and the gas stirring speed is 250 rpm for all of the experiments in the study. According to previous research[8] and the preliminary experiments, the temperature has no significant effect on the absorption rate; all of the experiments are performed at 30 °C and at atmospheric pressure.

3.3. Analytical Method. In the double-stirred tank reactor, the liquid-phase concentration is much larger than gas-phase concentration at the total reaction cycle. Thus, the liquid-phase concentration can be considered to be constant, and the absorption rate can also approximatively be considered to be constant in the absorption process. The inlet and outlet gases are analyzed for all of the experiments at 10 min because the absorption rate of the system remained stable after 7–8 min. The inlet and outlet gas concentrations of NO and NO_2 are measured simultaneously online using Testo 350 pro from Testo Instrumental Trading Co., Ltd., Shanghai, China.

4. Results and Discussion

4.1. Mass-Transfer Coefficient of the Gas and Liquid Films. The liquid-film mass-transfer coefficient (k_{LCO_2}) is determined by measuring the rate of physical absorption of pure CO_2 in water at 30 °C and then correlated to the liquid-phase stirring speed, n_L. Under these conditions, the gas-side mass-transfer coefficient is unimportant. Therefore, the liquid-film mass-transfer coefficient correlated to the liquid-phase stirring speed n_L is[23,24,41]

$$k_{LCO_2} = 1.075 \times 10^{-5} n_L^{0.544} \quad (23)$$

The gas-film mass-transfer coefficient (k_{GSO_2}) is determined by measuring the absorption rate of 2000 ppm SO_2 into 0.6 mol/L NaOH solution at 30 °C. In this case, the gas film diffusion is considered to be a rate-controlling step; that is, the gas-side mass-transfer coefficient determines the transfer rate. Therefore, the overall mass-transfer coefficient is approximately equal to the gas-side mass-transfer coefficient, $K_{GSO_2} = k_{GSO_2}$. In addition, the gas-side mass-transfer coefficient correlated to the gas-phase stirring speed n_G is[2,20,23,24]

$$k_{GSO_2} = 1.78 \times 10^{-6} n_G^{0.704} \quad (24)$$

The liquid- and gas-film mass-transfer coefficients of NO_2^* and NO* can be estimated by the following correlations involving the diffusivities of the compounds of interest and experimentally determined values of k_{LCO_2} and k_{GSO_2}, respectively.[20,24]
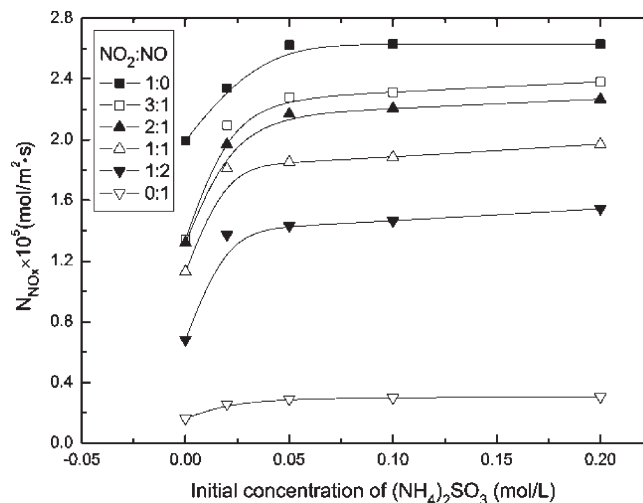
$$k_{LA} = k_{LCO_2}(D_{LA}/D_{LCO_2})^{2/3}, \quad (A = 1, 2) \quad (25)$$

$$k_{GA} = k_{GSO_2}(D_{GA}/D_{GSO_2})^{2/3}, \quad (A = 1, 2) \quad (26)$$

The values of D_{LCO_2} and D_{LA} ($A = 1, 2$), as shown in Table 3, are calculated through the equation of Wilke and Chang,[42] and the value of D_{GCO_2} and D_{GA} ($A = 1, 2$) for 30 °C, as shown in Table 3, is calculated through the formula of Maxwell–Gilliland[43] of eq 27.

$$D = \frac{4.36 \times 10^{-2} T^{3/2}(1/M_a + 1/M_b)^{1/2}}{P_0(v_a^{1/3} + v_b^{1/3})^2}, \quad (m^2/s) \quad (27)$$

The values of k_{GA} at 250 rpm and 30 °C and k_{LA} at 120 rpm and 30 °C calculated by eqs 25 and 26 are also shown in Table 3.

(41) Shi, Y.; Littlejohn, D.; Chang, S. G. *Environ. Sci. Technol.* **1996,** *30,* 3371–3376.
(42) Wilke, C. R.; Chang, P. *AIChE J.* **1955,** *1,* 264–270.
(43) McCabe, W. L.; Smith, J. C.; Harriott, P. *Unit Operations of Chemical Engineering*, 6th ed.; McGraw-Hill: New York, 2001.

Figure 2. Effect of the $(NH_4)_2SO_3$ concentration on the absorption rate (gas–liquid interfacial area, 50.27 cm²; T, 30 °C; inlet total concentration of NO + NO_2, 500 ppm).

Table 3. Physical Property of the Gas–Liquid Systems at 30 °C

	CO₂	SO₂	NO₂*	NO*
D_L (×10⁻⁹, m²/s)	2.319		2.423	2.887
D_G (×10⁻⁵, m²/s)		1.145	1.366	1.647
k_L (×10⁻⁴, m²/s)	1.454		1.497	1.682
k_G (×10⁻⁴, mol m⁻² s⁻¹ Pa⁻¹)		0.868	0.976	1.106

The value of Henry constants of NO_2^* can be calculated by eq 28,[44] and H_{NO^*} and H_{CO_2} can be calculated by the Henry law in eq 29[43]

$$H_{NO_2^*} = 1.2 \times 10^{-4} \exp\left[2500\left(\frac{1}{T} - \frac{1}{298}\right)\right],$$
$$(mol\ m^{-3}\ Pa^{-1}) \quad (28)$$

$$H_{NO^*} = \frac{\rho_{H_2O}}{E_{NO^*}M_{H_2O}}, \quad (mol\ m^{-3}\ Pa^{-1}) \quad (29)$$

where the Henry coefficient, $E_{NO^*} = 3.14 \times 10^6$ kPa at 30 °C.

4.2. Effect of the $(NH_4)_2SO_3$ Concentration on the NO_x Absorption Rate. A series of experiments are performed to investigate the effect of the $(NH_4)_2SO_3$ concentration on the NO_x absorption rate at different NO_2/NO ratios, while the NO_x partial pressure is 500 ppm. The experimental results shown in Figure 2 demonstrate that the NO_x absorption rate increases at different NO_2/NO ratios as the $(NH_4)_2SO_3$ concentration increases from 0 to 0.05 mol/L at 30 °C. This shows that the reaction is controlled concurrently by gas and liquid film. However, the NO_x absorption rate becomes nearly constant as the $(NH_4)_2SO_3$ concentration rises above 0.05 mol/L. In the latter case, the reaction may be mainly influenced by gas film and be zero-order with respect to the $(NH_4)_2SO_3$ concentration.
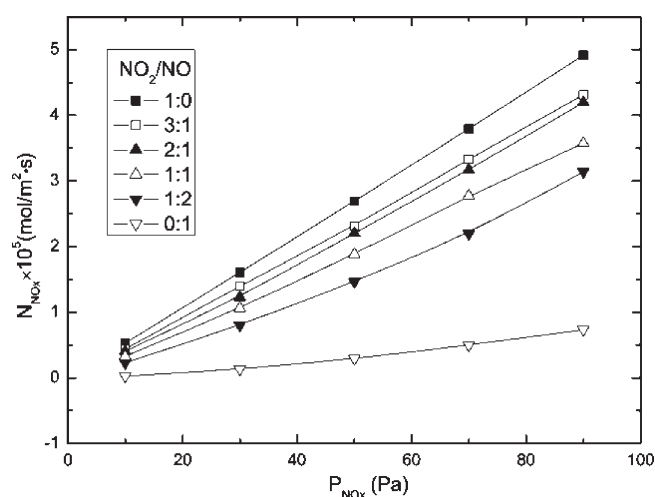
4.3. Effect of the Oxidation Degree on the NO_x Absorption Rate. Figure 3 shows the effect of NO_2/NO_x on the NO_x absorption rate at the $(NH_4)_2SO_3$ concentration of 0.1 mol/L. The total NO_x inlet concentration is 500 ppm, and the temperature is 30 °C. It is found that the NO_x absorption in $(NH_4)_2SO_3$ is strongly related to oxidation degree. The additions of the NO_2/NO_x result in a significant increase of the NO_x absorption rate. With the increase of the NO_2/NO_x ratio, the concentration of

(44) Mertes, S.; Wahner, A. *J. Phys. Chem.* **1995,** *99,* 14000–14006.
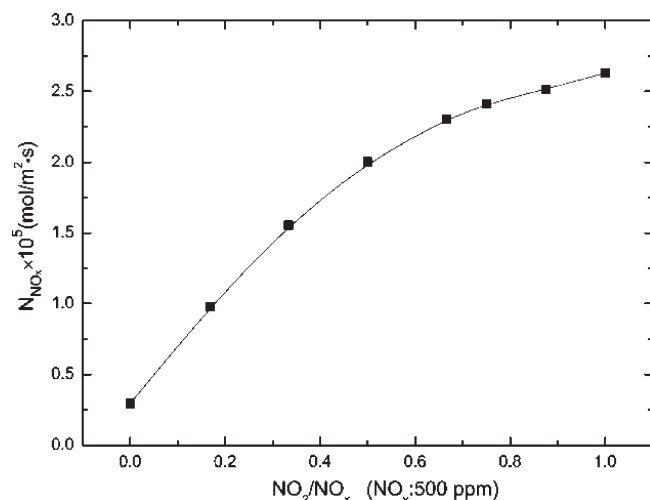
Figure 3. Effect of NO_2/NO_x on the NO_x absorption rate (gas−liquid interfacial area, 50.27 cm²; *T*, 30 °C; inlet total concentration of $NO + NO_2$, 500 ppm).

Figure 4. Effect of the NO_x partial pressure on the NO_x absorption rate [gas−liquid interfacial area, 50.27 cm²; *T*, 30 °C; $(NH_4)_2SO_3$, 0.1 mol/L].

NO_2 intensifies in the gas-phase equilibrium mixture, which can increase the equilibrium content of N_2O_4, and there is also an increase to a smaller extent in the N_2O_3 concentrations. Hence, the overall effect is that, with the increase of the NO_2/NO_x ratio and the dissolvable composition of N_2O_4 and N_2O_3 in the gas phase, the NO_x absorption rate rises.

4.4. Effect of the NO_x Partial Pressure on the NO_x Absorption Rate. Experiments are carried out at 30 °C and a $(NH_4)_2SO_3$ concentration of 0.1 mol/L to test the effect of NO_x partial pressures on the NO_x absorption rate. As the NO_x partial pressures increase from 10 to 90 Pa at different NO_2/NO ratios, the NO_x absorption rate increases. The experimental results shown in Figure 4 indicate that the absorption rate of NO_x into $(NH_4)_2SO_3$ solution increases with the increase of their partial pressure in the inlet gas. The relationship between the absorption rate of NO_x and the partial pressure of the inlet gas is nearly linear when the other parameters are held constant. This demonstrates that the reactions are always limited by gas-film resistances and the increasing NO_x partial pressures enhance the driving force for their absorption in the gas side.
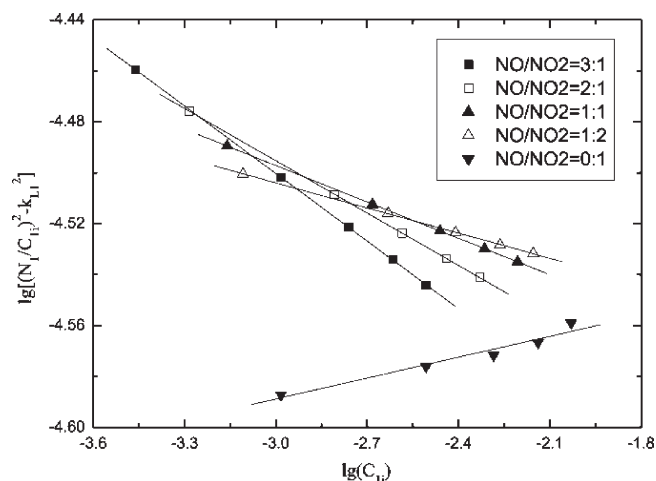
Figure 5. Plot of $\log[(N_1/C_{1i})^2 - k_{L1}^2]$ versus $\log(C_{1i})$.

4.5. Analysis of Experimental Data. As shown in Figure 2, when the $(NH_4)_2SO_3$ concentration is above 0.05 mol/L, the effect of C_{BL} on the NO_x absorption rate is not significant. Therefore, the reactions 11 and 12 are considered zero-order with respect to the $(NH_4)_2SO_3$ concentration, and the value of *n* in eq 21 is 0 in this case. Equation 21 can be expressed as

$$\left[\frac{N_A k_{GA}}{(P_A k_{GA} - N_A)H_A}\right]^2 - k_{LA}^2$$
$$= \frac{2}{m_A + 1}k_{Am,n}D_{LA}C_{Ai}^{m_A - 1}, \quad (A = 1, 2) \quad (30)$$

In combination with eq 15, eq 30 can be rewritten as

$$\left(\frac{N_A}{C_{Ai}}\right)^2 - k_{LA}^2 = \frac{2}{m_A + 1}k_{Am,n}D_{LA}C_{Ai}^{m_A - 1},$$
$$(A = 1, 2) \quad (31)$$

In addition, eq 31 can be written in logarithmic form as follows:

$$\log\left[\left(\frac{N_A}{C_{Ai}}\right)^2 - k_{LA}^2\right] = (m_A - 1)\log C_{Ai}$$
$$+ \log\left(\frac{2}{m_A + 1}k_{Am,n}D_{LA}\right), \quad (A = 1, 2) \quad (32)$$

With the relations of $N_A = k_{GA}(P_A - P_{Ai})$ and $C_{Ai} = P_{Ai}/H$, the value of C_{Ai} can be calculated by

$$C_{Ai} = \left(P_A - \frac{Q(C_{A1} - C_{A2})}{k_{GA}S}\right)/H_A \quad (33)$$

Because the composition of NO_x is characterized by the two chemical species NO_2^* and NO^* and the inlet and outlet partial pressures of NO_2^* and NO^* can be gained through eqs 9 and 10, the absorption rates of NO_2^* and NO^* can be gained by eq 13. Then, using data in Figure 4 and eqs 32 and 33, the relationship between $\log\left[\left(\frac{N_A}{C_{Ai}}\right)^2 - k_{LA}^2\right]$ and $\log C_{Ai}$ can be obtained and are shown in Figure 5 and Figure 6. There is a linear relationship between $\log[(N_A/C_{Ai})^2 - k_{LA}^2]$ and $\log C_{Ai}$. The slope of the fit lines at different NO_2/NO ratios and the value of m_A (*A* = 1, 2) are shown in Table 4. Through eq 31, $k_{Am,n}$ (*A* = 1, 2) can be calculated, as seen in Table 4.
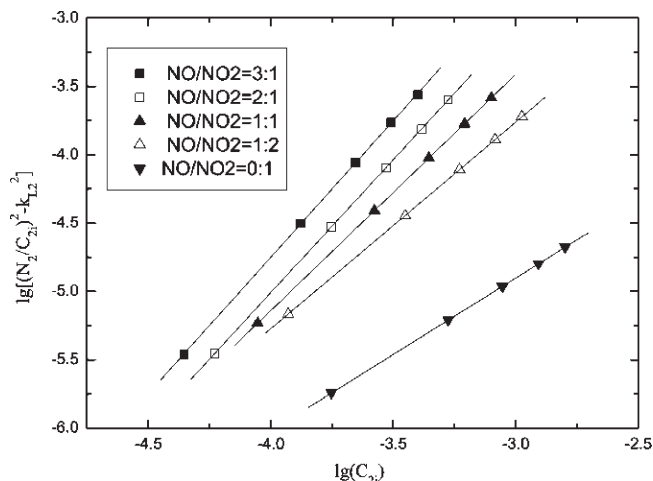
Figure 6. Plot of $\log[(N_2/C_{2i})^2 - k_{L2}^2]$ versus $\log(C_{2i})$.
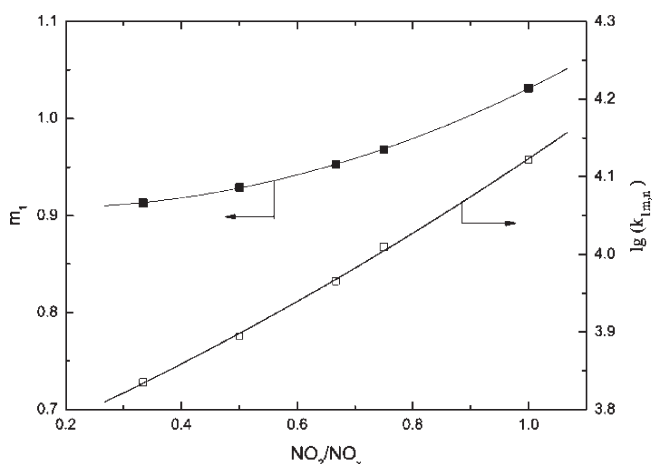
Figure 7. Plot of m_1 and $k_{1m,n}$ for NO_2^* versus NO_2/NO_x.

Table 4. Values of m_A and $k_{Am,n}$ for Different NO_2/NO Ratios

NO_2/NO	Φ	m_1	m_2	$k_{1m,n}$	$k_{2m,n}$
1:0	1	1.031		1.32×10^4	
3:1	0.75	0.968	2.994	1.02×10^4	1.15×10^{12}
2:1	0.667	0.953	2.938	9.24×10^3	3.84×10^{11}
1:1	0.5	0.929	2.724	7.84×10^3	3.72×10^{10}
1:2	0.333	0.913	2.509	6.85×10^3	3.54×10^9
0:1	0		2.118		1.52×10^7

Clearly, at different NO_2/NO ratios, the orders of reactions with respect to the concentration of NO_2^* and NO^* in the gas phase and the reaction rate constants of NO_2^* and NO^* with the $(NH_4)_2SO_3$ solution are different, and using the data in Table 4, the plot of m_1 and $\log(k_{1m,n})$ versus the oxidation degree (Φ) and the plot of m_2 and $\log(k_{2m,n})$ versus the oxidation degree (Φ) are produced, as shown in Figures 7 and 8, respectively.

The values of m_A and $k_{Am,n}$ ($A = 1, 2$) are the function of the oxidation degree (Φ) and may be represented by the equation as follows:

$$m_1 = 0.174\Phi^2 - 0.055\Phi + 0.912 \tag{34}$$

$$m_2 = 0.231\Phi^2 + 1.093\Phi + 2.120 \tag{35}$$

$$k_{1m,n} = 10^{0.096\Phi^2 + 0.306\Phi + 3.721} \tag{36}$$
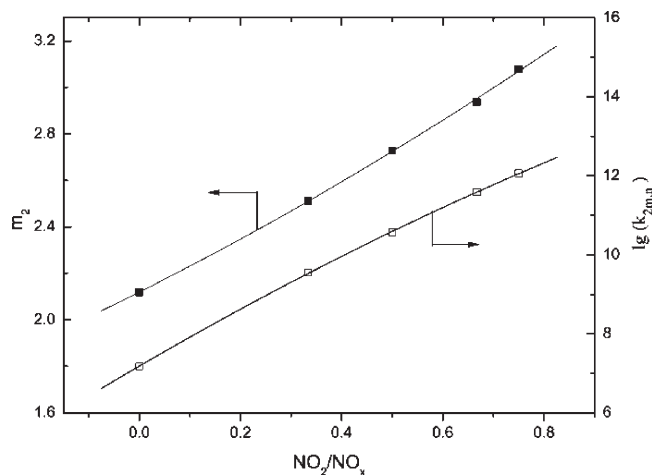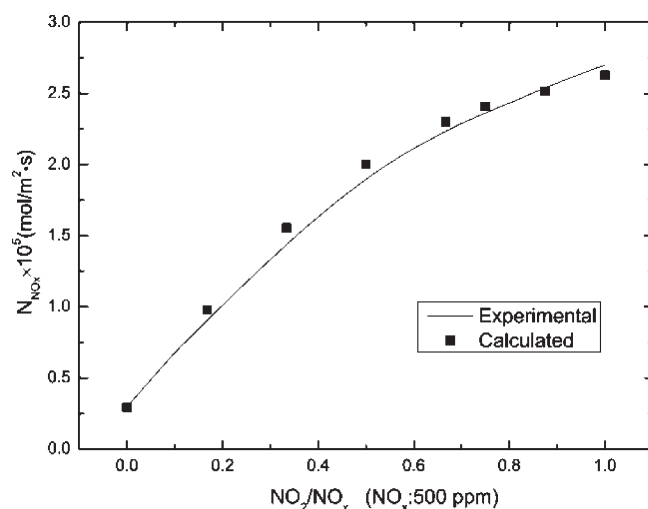
$$k_{2m,n} = 10^{-1.292\Phi^2 + 7.461\Phi + 7.185} \tag{37}$$

Figure 8. Plot of m_2 and $k_{2m,n}$ for NO^* versus NO_2/NO_x.

Figure 9. Comparison between the experimental and calculated values.

Using eqs 34−37, the total absorption rate of NO_x into $(NH_4)_2SO_3$ solution may be represented by the following equation:

$$N_A = ((\Phi P_{NO_x})/((1/k_{G1}) + (1/(H_1(k_{L1}^2 + (2/0.174\Phi^2 - 0.055\Phi$$
$$+ 1.912)10^{0.096\Phi^2 + 0.306\Phi + 3.721}D_{L1}C_{1i}^{0.174\Phi^2 - 0.055\Phi - 0.088})^{-1}))))$$
$$+ (((1-\Phi)P_{NO_x})/((1/k_{G2}) + (1/(H_2(k_{L2}^2 + (2/0.231\Phi^2 + 1.093\Phi$$
$$+ 3.120)10^{-1.292\Phi^2 + 7.461\Phi + 7.185}D_{L2}C_{2i}^{0.231\Phi^2 + 1.093\Phi + 1.120})^{-1}))))$$
$$\tag{38}$$

The comparison between calculated values by eq 38 and experimental values of the NO_x absorption rate for different oxidation degrees (Φ) can be found in Figure 9. It can be seen that the calculated values fit the experimental data well.

5. Conclusions

The absorption kinetics of NO_x into the aqueous $(NH_4)_2$-SO_3 solution has been studied in a double-stirred reactor. The following specific conclusions can be drawn from the experimental results: (1) The gas−liquid reaction between NO_x and $(NH_4)_2SO_3$ is controlled by both the gas and liquid films because the $(NH_4)_2SO_3$ concentration is lower than 0.05 mol/L, but it is mainly controlled by the gas film at higher concentrations.

In the latter case, the absorption rates are found to be zero-order with respect to the $(NH_4)_2SO_3$ concentration. (2) The absorption rates of NO* and NO_2* increase with the rise of their partial pressures in the inlet gas, and the NO_x absorption rate increases as the NO_2/NO_x ratio increases. (3) The orders of the reaction with respect to the concentration of NO_2* and NO* in bulk gas and the reaction rate constants of NO_2* and NO* with $(NH_4)_2SO_3$ are all the function of the oxidation degree (Φ). In addition, the kinetic equation for NO_x absorption as a function of the oxidation degree can be written as

$$N_A = ((\Phi P_{NO_x})/((1/k_{G1}) + (1/(H_1(k_{L1}^2 + (2/0.174\Phi^2 - 0.055\Phi$$
$$+ 1.912)10^{0.096\Phi^2 + 0.306\Phi + 3.721} D_{L1} C_{1i}^{0.174\Phi^2 - 0.055\Phi - 0.088})^{-1}))))$$
$$+ (((1 - \Phi)P_{NO_x})/((1/k_{G2}) + (1/(H_2(k_{L2}^2 + (2/0.231\Phi^2 + 1.093\Phi$$
$$+ 3.120)10^{-1.292\Phi^2 + 7.461\Phi + 7.185} D_{L2} C_{2i}^{0.231\Phi^2 + 1.093\Phi + 1.120})^{-1}))))$$

Nomenclature

S = interfacial area (m^2)
C_{A1} = A concentration of inlet gas (mol m^{-3})
C_{A2} = A concentration of outlet gas (mol m^{-3})
C_{Ai} = A concentration at the interface (mol m^{-3})
C_{AL} = A concentration in the bulk of liquid (mol m^{-3})
C_{BL} = $(NH_4)_2SO_3$ concentration in the bulk of liquid (mol m^{-3})
D_{LCO_2} = diffusivity of CO_2 in water ($m^2 s^{-1}$)
D_{LA} = diffusivity of A in water ($m^2 s^{-1}$)
D_{GSO_2} = diffusivity of SO_2 in air ($m^2 s^{-1}$)
D_{GA} = diffusivity of A in air ($m^2 s^{-1}$)
E = enhancement factor
E_∞ = enhancement factor when the reaction is instantaneous

γ_L = conversion coefficient in liquid film
H_A = solubility coefficient (mol m^{-3} Pa^{-1})
H_i = solubility coefficient (mol m^{-3} Pa^{-1})
k_{GA} = gas-phase mass-transfer coefficient (mol $m^{-2} s^{-1}$ Pa^{-1})
k_{LA} = liquid-phase mass-transfer coefficient (m s^{-1})
K_G = overall mass-transfer coefficient in the gas phase (mol $m^{-2} s^{-1}$ Pa^{-1})
N_A = absorption rate of A (mol $m^{-2} s^{-1}$)
P_A = partial pressure of A in the bulk of gas (Pa)
P_{Ai} = partial pressure of A at the interface (Pa)
P_{NO_x} = partial pressure of NO_x (Pa)
P_0 = total pressure (Pa)
P_I = partial pressure of inerts (Pa)
Q = gas flow rate ($m^3 s^{-1}$)
R = gas constant (8.314 J mol^{-1} K^{-1})
v_G = gas volume rate ($m^3 s^{-1}$)
$k_{Am,n}$ = rate constant of A
K_1 and K_2 = equilibrium constants of A
NO* = inferior nitrogen oxides ($NO + N_2O_3$)
NO_2* = superior nitrogen oxides ($NO_2 + N_2O_3 + 2N_2O_4$)
NO_x = total nitrogen oxides (NO* + NO_2*)
T = temperature (K)
M_a and M_b = molecular weights of a and b (g mol^{-1})
v_a and v_b = molecular volumes of a and b ($cm^3 mol^{-1}$)
m_A = order of the reaction with respect to the concentration of A in the bulk gas
n_A = order of the reaction with respect to the concentration of $(NH_4)_2SO_3$
E_{NO*} = Henry coefficient of NO (kPa)
ρ_{H_2O} = density of H_2O (kg m^{-3})
M_{H_2O} = molecular weight of H_2O (g mol^{-1})

Subscripts

in = inlet of the gas stream
out = outlet of the gas stream
A = 1 and 2, where A = 1 is NO_2* and A = 2 is NO*